On the Linear Convergence of the ADMM in Decentralized Consensus Optimization

Wei Shi, Qing Ling, Kun Yuan, Gang Wu, and Wotao Yin

Abstract

In decentralized consensus optimization, a connected network of agents collaboratively minimize the sum of their local objective functions over a common decision variable, where their information exchange is restricted between the neighbors. To this end, one can first obtain a problem reformulation and then apply the alternating direction method of multipliers (ADMM). The method applies iterative computation at the individual agents and information exchange between the neighbors. This approach has been observed to converge quickly and deemed powerful. This paper establishes its linear convergence rate for the decentralized consensus optimization problem with strongly convex local objective functions. The theoretical convergence rate is explicitly given in terms of the network topology, the properties of local objective functions, and the algorithm parameter. This result is not only a performance guarantee but also a guideline toward accelerating the ADMM convergence.

Index Terms

Decentralized consensus optimization, alternating direction method of multipliers (ADMM), linear convergence

I. INTRODUCTION

Recent advances in signal processing and control of networked multi-agent systems have led to much research interests in decentralized optimization [2]–[14]. Decentralized optimization problems arising in networked multi-agent systems include coordination of aircraft or vehicle networks [2]–[4], data processing of wireless sensor networks [5]–[10], spectrum sensing of cognitive radio networks [11], [12], state estimation and operation optimization of smart grids [13], [14], etc. In these scenarios, the data is collected and/or stored in a distributed manner; a fusion center is either disallowed or not economical. Consequently, any computing tasks must be accomplished in a decentralized and collaborative manner by the agents. This approach can be powerful and efficient, as the computing tasks are distributed over all the agents and information exchange occurs only between the agents with direct communication links. There is no risk of central computation overload or network congestion.

In this paper, we focus on *decentralized consensus optimization*, an important class of decentralized optimization in which a network of L agents cooperatively solve

$$\min_{\tilde{x}} \quad \sum_{i=1}^{L} f_i(\tilde{x}), \tag{1}$$

over a common optimization variable $\tilde{x}$, where $f_i(\tilde{x}) : \mathbb{R}^N \to \mathbb{R}$ is the local objective function known by agent i. This formulation arises in averaging [4]–[6], learning [7], [8], and estimation [9]–[13] problems. Examples of $f_i(\tilde{x})$ include least squares [4]–[6], regularized least squares [8], [10]–[12], as well as more general ones [7]. The values of $\tilde{x}$ can stand for average temperature of a room [5], [6], frequency-domain occupancy of spectra [11], [12], states of a smart grid system [13], [14], and so on.

There exist several methods for decentralized consensus optimization, including distributed subgradient descent algorithms [15]–[17], dual averaging methods [18], [19], and the alternating direction method of multipliers (ADMM) [8]–[10], [20], [21]. Among these algorithms, the ADMM demonstrates fast convergence in many applications, e.g., [8]–[10]. However, how fast it converges and what factors affect the rate are both unknown. This paper addresses these issues.

A. Our Contributions

Firstly, we establish the linear convergence rate of the ADMM that is applied to decentralized consensus optimization with strongly convex local objective functions. This theoretical result gives a performance guarantee for the ADMM and validates the observation in prior literature.

Secondly, we study how the network topology, the properties of local objective functions, and the algorithm parameter affect the convergence rate. The analysis provide guidelines for networking strategies,

objective-function splitting strategies, and algorithm parameter settings to achieve faster convergence.

B. Related Work

Besides the ADMM, existing decentralized approaches for solving (1) include belief propagation [7], incremental optimization [22], subgradient descent [15]–[17], dual averaging [18], [19], etc. Belief propagation and incremental optimization require one to predefine a tree or loop structure in the network, whereas the advantage of the ADMM, subgradient descent, and dual averaging is that they do not rely on any predefined structures. Subgradient descent and dual averaging work well for asynchronous networks but suffer from slow convergence. Indeed, for subgradient descent algorithms [15] and [16] establish the convergence rate of $O(1/k)$, where k is the number of iterations, to a neighborhood of the optimal solution when the local subgradients are bounded and the stepsize is fixed. Further assuming that the local objective functions are strongly convex, choosing a dynamic stepsize leads to a rate of $O(\log(k)/k)$ [17]. Dual averaging methods using dynamic stepsizes also have sublinear rates, e.g., $O(\log(k)/\sqrt{k})$ as proved in [18] and [19].

The decentralized ADMM approaches use synchronous steps by all the agents but have much faster empirical convergence, as demonstrated in many applications [8]–[10]. However, existing convergence rate analysis of the ADMM is restricted to the classic, centralized computation. The centralized ADMM has a sublinear convergence rate $O(1/k)$ for general convex optimization problems [23]. In [24] an ADMM with restricted stepsizes is proposed and proved to be linearly convergent for certain types of non-strongly convex objective functions. A recent paper [25] shows a linear convergence rate $O(1/a^k)$ for some $a > 1$ under a strongly convex assumption, and our paper extends the analysis tools therein to the decentralized regime.

A notable work about convergence rate analysis is [20], which proves the linear convergence rate of the ADMM applied to the average consensus problem, a special case of (1) in which $f_i(\tilde{x}) = \|\tilde{x} - y_i\|_2^2$ with y_i being a local measurement vector of agent i. Its analysis takes a state-transition equation approach, which is not applicable to the more general local objective functions considered in this paper.

C. Paper Organization and Notation

This paper is organized as follows. Section II reformulates the decentralized consensus optimization problem and develops an algorithm based on the ADMM. Section III analyzes the linear convergence rate of the ADMM and shows how to accelerate the convergence through tuning the algorithm parameter.

Section IV provides extensive numerical experiments to validate the theoretical analysis in Section III. Section V concludes the paper.

In this paper we denote $\|x\|_2$ as the Euclidean norm of a vector x and $\langle x, y \rangle$ as the inner product of two vectors x and y. Given a semidefinite matrix G with proper dimensions, the G-norm of x is $\sqrt{x^T G x}$. We let $\sigma_{\max}(G)$ be the operator that returns the largest singular value of G and $\tilde{\sigma}_{\min}(G)$ be the one that returns the smallest nonzero singular value of G.

We use two kinds of definitions of convergence, Q-linear convergence and R-linear convergence. We say that a sequence y^k, where the superscript k stands for time index, Q-linearly converges to a point y^* if there exists a number $\rho \in (0, 1)$ such that $\lim\limits_{k \to \infty} \frac{\|y^{k+1} - y^*\|}{\|y^k - y^*\|} = \rho$ with $\| \cdot \|$ being a vector norm. We say that a sequence x^k R-linearly converges to a point x^* if for all k, $\|x^k - x^*\| \leq \|y^k - y^*\|$ where y^k Q-linearly converges to y^*.

II. The ADMM for Decentralized Consensus Optimization

In this section, we first reformulate the decentralized consensus optimization problem (1) such that it can be solved by the ADMM (see Section II-A). Then we develop the decentralized ADMM approach and provide a simplified decentralized algorithm (see Section II-B).

A. Problem Formulation

Throughout the paper, we consider a network consisting of L agents bidirectionally connected by E edges (and thus $2E$ arcs). We can describe the network as a symmetric directed graph $\mathcal{G}_d = \{\mathcal{V}, \mathcal{A}\}$ or an undirected graph $\mathcal{G}_u = \{\mathcal{V}, \mathcal{E}\}$, where $\mathcal{V}$ is the set of vertexes with cardinality $|\mathcal{V}| = L$, $\mathcal{A}$ is the set of arcs with $|\mathcal{A}| = 2E$, and $\mathcal{E}$ is the set of edges with $|\mathcal{E}| = E$. Algorithms that solve the decentralized consensus optimization problem (1) are developed based on this graph.

Generally speaking, the ADMM applies to the convex optimization problem in the form of

$$\begin{aligned} \min_{y_1, y_2} \quad & g_1(y_1) + g_2(y_2), \\ \text{s.t.} \quad & C_1 y_1 + C_2 y_2 = b, \end{aligned} \tag{2}$$

where y_1 and y_2 are optimization variables, g_1 and g_2 are convex functions, and $C_1 y_1 + C_2 y_2 = b$ is a linear constraint of y_1 and y_2. The ADMM solves a sequence of subproblems involving g_1 and g_2 one at a time and iterates to converge as long as a saddle point exists.

To solve (1) with the ADMM in a decentralized manner, we reformulate it as

$$\begin{aligned} \min_{\{x_i\}, \{z_{ij}\}} \quad & \sum_{i=1}^{L} f_i(x_i), \\ \text{s.t.} \quad & x_i = z_{ij}, \ x_j = z_{ij}, \ \forall (i, j) \in \mathcal{A}. \end{aligned} \tag{3}$$

Here x_i is the local copy of the common optimization variable $\tilde{x}$ at agent i and z_{ij} is an auxiliary variable imposing the consensus constraint on neighboring agents i and j. In the constraints, $\{x_i\}$ are separable when $\{z_{ij}\}$ are fixed, and vice versa. Therefore, (3) lends itself to decentralized computation in the ADMM framework. Apparently, (3) is equivalent to (1) when the network is connected.

Defining $x \in \mathbb{R}^{LN}$ as a vector concatenating all x_i, $z \in \mathbb{R}^{2EN}$ as a vector concatenating all z_{ij}, and $f(x) = \sum_{i=1}^{L} f_i(x_i)$, (3) can be written in a matrix form as

$$
\begin{aligned}
\min_{x,z} \quad & f(x) + g(z), \\
\text{s.t.} \quad & Ax + Bz = 0,
\end{aligned}
\tag{4}
$$

where $g(z) = 0$, which fits the form of (2), and is amenable to the ADMM. Here $A = [A_1; A_2]$; $A_1, A_2 \in \mathbb{R}^{2EN \times LN}$ are both composed of $2E \times L$ blocks of $N \times N$ matrices. If $(i,j) \in \mathcal{A}$ and z_{ij} is the qth block of z, then the (q,i)th block of A_1 and the (q,j)th block of A_2 are $N \times N$ identity matrices I_N; otherwise the corresponding blocks are $N \times N$ zero matrices 0_N. Also, we have $B = [-I_{2EN}; -I_{2EN}]$ with I_{2EN} being a $2EN \times 2EN$ identity matrix.

B. Algorithm Development

Now we apply the ADMM to solve (4). The augmented Lagrangian of (4) is

$$
L_c(x, z, \lambda) = f(x) + \langle \lambda, Ax + Bz \rangle + \frac{c}{2} \|Ax + Bz\|_2^2,
$$

where $\lambda \in \mathbb{R}^{4EN}$ is the Lagrange multiplier and c is a positive algorithm parameter. At iteration $k + 1$, the ADMM firstly minimizes $L_c(x, z^k, \lambda^k)$ to obtain x^{k+1}, secondly minimizes $L_c(x^{k+1}, z, \lambda^k)$ to obtain z^{k+1}, and finally updates λ^{k+1} from x^{k+1} and z^{k+1}. The updates are

$$
\begin{aligned}
x\text{-update:} \quad & \nabla f(x^{k+1}) + A^T \lambda^k + cA^T(Ax^{k+1} + Bz^k) = 0, \\
z\text{-update:} \quad & B^T \lambda^k + cB^T(Ax^{k+1} + Bz^{k+1}) = 0, \\
\lambda\text{-update:} \quad & \lambda^{k+1} - \lambda^k - c(Ax^{k+1} + Bz^{k+1}) = 0,
\end{aligned}
\tag{5}
$$

where $\nabla f(x^{k+1})$ is the gradient of $f(x)$ at point $x = x^{k+1}$ if f is differentiable, or is a subgradient if f is non-differentiable.

Next we show that if the initial values of z and λ are properly chosen the ADMM updates in (5) can be simplified (see also the derivation in [8]). Multiplying the two sides of the λ-update by A^T and adding it to the x-update, we have $\nabla f(x^{k+1}) + A^T \lambda^{k+1} + cA^T B(z^k - z^{k+1}) = 0$. Further, multiplying the two sides of the λ-update by B^T and adding it to the z-update we have $B^T \lambda^{k+1} = 0$. Therefore (5)

can be equivalently expressed as

$$\nabla f(x^{k+1}) + A^T \lambda^{k+1} + cA^T B(z^k - z^{k+1}) = 0,$$
$$B^T \lambda^{k+1} = 0, \qquad (6)$$
$$\lambda^{k+1} - \lambda^k - c(Ax^{k+1} + Bz^{k+1}) = 0.$$

Letting $\lambda = [\beta; \gamma]$ with $\beta, \gamma \in \mathbb{R}^{2EN}$ and recalling $B = [-I_{2EN}; -I_{2EN}]$, we know $\beta^{k+1} = -\gamma^{k+1}$ from the second equation of (6). Therefore, the first equation in (6) reduces to $\nabla f(x^{k+1}) + M_- \beta^{k+1} - cM_+(z^k - z^{k+1}) = 0$ where $M_+ = A_1^T + A_2^T$ and $M_- = A_1^T - A_2^T$. The third equation in (6) splits to two equations $\beta^{k+1} - \beta^k - cA_1 x^{k+1} + cz^{k+1} = 0$ and $\gamma^{k+1} - \gamma^k - cA_2 x^{k+1} + cz^{k+1} = 0$. If we choose the initial value of λ as $\beta^0 = -\gamma^0$ such that $\beta^k = -\gamma^k$ holds for $k = 0, 1, \cdots$, summing and subtracting these two equations result in $\frac{1}{2} M_+^T x^{k+1} - z^{k+1} = 0$ and $\beta^{k+1} - \beta^k - \frac{c}{2} M_-^T x^{k+1} = 0$, respectively. If we further choose the initial value of z as $z^0 = \frac{1}{2} M_+^T x^0$, $\frac{1}{2} M_+^T x^k - z^k = 0$ holds for $k = 0, 1, \cdots$.

To summarize, with initialization $\beta^0 = -\gamma^0$ and $z^0 = \frac{1}{2} M_+^T x^0$, (6) reduces to

$$\nabla f(x^{k+1}) + M_- \beta^{k+1} - cM_+(z^k - z^{k+1}) = 0,$$
$$\beta^{k+1} - \beta^k - \frac{c}{2} M_-^T x^{k+1} = 0, \qquad (7)$$
$$\frac{1}{2} M_+^T x^k - z^k = 0.$$

In Section III we will analyze the convergence rate of the ADMM updates (7). The analysis requires an extra initialization condition that β^0 lies in the column space of M_-^T (e.g., $\beta^0 = 0$) such that β^{k+1} also lies in the column space of M_-^T; the reason will be given in Section III.

Indeed, (7) also leads to a simple decentralized algorithm that involves only an x-update and a new multiplier update. To see this, substituting $\frac{1}{2} M_+^T x^k - z^k = 0$ into the first two equations of (7) we have

$$\nabla f(x^{k+1}) + M_- \beta^{k+1} - \frac{c}{2} M_+ M_+^T x^k + \frac{c}{2} M_+ M_+^T x^{k+1} = 0,$$
$$\beta^{k+1} - \beta^k - \frac{c}{2} M_-^T x^{k+1} = 0, \qquad (8)$$

which is irrelevant with z. Note that in the first equation of (8) the x-update relies on $M_- \beta^{k+1}$ other than β^k. Therefore, multiplying the second equation with M_- we have $M_- \beta^{k+1} - M_- \beta^k - \frac{c}{2} M_- M_-^T x^{k+1} = 0$. Substituting it to the first equation of (8) we obtain the x-update where x^{k+1} is decided by x^k and $M_- \beta^k$, i.e., $\nabla f(x^{k+1}) + M_- \beta^k + (\frac{c}{2} M_+ M_+^T + \frac{c}{2} M_- M_-^T) x^{k+1} - \frac{c}{2} M_+ M_+^T x^k = 0$. Letting $W \in \mathbb{R}^{LN \times LN}$ be a block diagonal matrix with its (i,i)th block being the degree of agent i multiplying I_N and other blocks being 0_N, $L_+ = \frac{1}{2} M_+ M_+^T$, $L_- = \frac{1}{2} M_- M_-^T$, we know $W = \frac{1}{2}(L_+ + L_-)$. Defining a new multiplier $\alpha = M_- \beta \in \mathbb{R}^{LN}$, we obtain a simplified decentralized algorithm

$$x\text{-update:} \quad \nabla f(x^{k+1}) + \alpha^k + 2cW x^{k+1} - cL_+ x^k = 0,$$
$$\alpha\text{-update:} \qquad \qquad \alpha^{k+1} - \alpha^k - cL_- x^{k+1} = 0. \qquad (9)$$

TABLE I

ALGORITHM 1: DECENTRALIZED CONSENSUS OPTIMIZATION BASED ON THE ADMM

Input functions f_i; initialize variables $x_i^0 = 0$, $\alpha_i^0 = 0$; set algorithm parameter $c > 0$;

For $k = 0, 1, \cdots$, every agent i do

    Update x_i^{k+1} by solving $\nabla f_i(x_i^{k+1}) + \alpha_i^k + 2c|\mathcal{N}_i|x_i^{k+1} - c\left(|\mathcal{N}_i|x_i^k + \sum_{j \in \mathcal{N}_i} x_j^k\right) = 0$;

    Update $\alpha_i^{k+1} = \alpha_i^k + c\left(|\mathcal{N}_i|x_i^{k+1} - \sum_{j \in \mathcal{N}_i} x_j^{k+1}\right)$;

End for

The introduced matrices M_+, M_-, L_+, L_-, and W are related to the underlying network topology. With regard to the undirected graph $\mathcal{G}_\mathrm{u}$, M_+ and M_- are the extended unoriented and oriented incidence matrices, respectively; L_+ and L_- are the extended signless and signed Laplacian matrices, respectively; and W is the extended degree matrix. By "extended", we mean replacing every 1 by I_N, -1 by $-I_N$, and 0 by 0_N in the original definitions of these matrices [26]–[29].

The updates in (9) are distributed to agents. Note that $x = [x_1; \cdots; x_L]$ where x_i is the local solution of agent i and $\alpha = [\alpha_1; \cdots; \alpha_L]$ where $\alpha_i \in \mathbb{R}^N$ is the local Lagrange multiplier of agent i. Recalling the definitions of W, L_+ and L_-, (9) translates the update of agent i by

$$\nabla f_i(x_i^{k+1}) + \alpha_i^k + 2c|\mathcal{N}_i|x_i^{k+1} - c\left(|\mathcal{N}_i|x_i^k + \sum_{j \in \mathcal{N}_i} x_j^k\right) = 0,$$
$$\alpha_i^{k+1} = \alpha_i^k + c\left(|\mathcal{N}_i|x_i^{k+1} - \sum_{j \in \mathcal{N}_i} x_j^{k+1}\right),$$

(10)

where $\mathcal{N}_i$ denotes the set of neighbors of agent i. The algorithm is fully decentralized since the updates of x_i and α_i only rely on local and neighboring information. The decentralized consensus optimization algorithm based on the ADMM is outlined in Table I.

III. CONVERGENCE RATE ANALYSIS

This section first establishes the linear convergence rate of the ADMM in decentralized consensus optimization with strongly convex local objective functions (see Section III-A); the detailed proof of the main theoretical result is placed in Appendix. We then discuss how to tune the parameter and accelerate the convergence (see Section III-B).

A. Main Theoretical Result

Throughout this paper, we make the following assumption that the local objective functions are strongly convex and have Lipschitz continuous gradients; note that the latter implies differentiability.

Assumption 1. *The local objective functions are strongly convex. For each agent i and given any $\tilde{x}_a, \tilde{x}_b \in \mathbb{R}^N$ $\langle \nabla f_i(\tilde{x}_a) - \nabla f_i(\tilde{x}_b), \tilde{x}_a - \tilde{x}_b \rangle \geq m_{f_i} \|\tilde{x}_a - \tilde{x}_b\|_2^2$ with $m_{f_i} > 0$. The gradients of the local objective functions are Lipschitz continuous. For each agent i and given any $\tilde{x}_a, \tilde{x}_b \in \mathbb{R}^N$, $\|\nabla f_i(\tilde{x}_a) - \nabla f_i(\tilde{x}_b)\|_2 \leq M_{f_i} \|\tilde{x}_a - \tilde{x}_b\|_2$ with $M_{f_i} > 0$.*

Recall the definition $f(x) = \sum_{i=1}^{L} f_i(x_i)$. Assumption 1 directly indicates that $f(x)$ is strongly convex (i.e., $\langle \nabla f(x_a) - \nabla f(x_b), x_a - x_b \rangle \geq m_f \|x_a - x_b\|_2^2$ given any $x_a, x_b \in \mathbb{R}^{LN}$ with $m_f = \min_i m_{f_i}$) and the gradient of $f(x)$ is Lipschitz continuous (i.e., $\|\nabla f(x_a) - \nabla f(x_b)\|_2 \leq M_f \|x_a - x_b\|_2$ for any $x_a, x_b \in \mathbb{R}^{LN}$ with $M_f = \max_i M_{f_i}$).

Although the convergence of Algorithm 1 to the optimal solution of (4) can be shown based on the convergence property of the ADMM (see e.g., [21]), establishing its linear convergence is nontrivial. In [25] the linear convergence of the centralized ADMM is proved given that either $g(z)$ is strongly convex or B is full row-rank in (4). However, the decentralized consensus optimization problem does not satisfy these conditions. The function $g(z) = 0$ is not strongly convex, and the matrix $B = [-I_{2EN}; -I_{2EN}]$ is row-rank deficient.

Next we will analyze the convergence rate of the ADMM iteration (7). The analysis requires an extra initialization condition that β^0 lies in the column space of M_-^T such that β^{k+1} also lies in the column space of M_-^T, which is necessary in the analysis. Note that there is a unique optimal multiplier β^* lying in the column space of M_-^T. To see so, consider the KKT conditions of (4)

$$
\begin{aligned}
\nabla f(x^*) + M_- \beta^* &= 0, \\
M_-^T x^* &= 0, \\
\tfrac{1}{2} M_+^T x^* - z^* &= 0,
\end{aligned}
\tag{11}
$$

where (x^*, z^*) is the unique primal optimal solution and the uniqueness follows from the strong convexity of $f(x)$ as well as the consensus constraint $Ax + Bz = 0$. Since the consensus constraints $Ax + Bz = 0$ are feasible, there is at least one optimal multiplier $\tilde{\beta}$ exists such that $\nabla f(x^*) + M_- \tilde{\beta} = 0$. We show that its projection onto the column space of M_-^T, denoted by β^*, is also an optimal multiplier. According to the property of projection, $M_-(\tilde{\beta} - \beta^*) = 0$ and hence $M_- \tilde{\beta} = M_- \beta^*$. Therefore, the projection β^* that lies in the column space of M_-^T also satisfies $\nabla f(x^*) + M_- \beta^* = 0$. Next we show the uniqueness of such a β^* by

contradiction. Consider two different vectors $M_-^T v_1, M_-^T v_2 \in \mathbb{R}^{2EN}$ that both lie in the column space of M_-^T and satisfy the equation. Therefore, we have $\nabla f(x^*) + M_- M_-^T v_1 = 0$ and $\nabla f(x^*) + M_- M_-^T v_2 = 0$. Subtracting them yields $M_- M_-^T (v_1 - v_2) = 0$. Since $\|M_- M_-^T (v_1 - v_2)\|_2 \geq \tilde{\sigma}_{\min}(M_-)\|M_-^T(v_1 - v_2)\|_2$ where $\tilde{\sigma}_{\min}(M_-)$ is the smallest nonzero singular value of M_-, we conclude that $\|M_-^T(v_1 - v_2)\|_2 = 0$ and consequently $M_-^T v_1 = M_-^T v_2$ which contradicts with the assumption of $M_-^T v_1$ and $M_-^T v_2$ being different. Hence, β^* is the unique dual optimal solution that lies in the column space of M_-^T.

Our main theoretical result considers the convergence of a vector that concatenating the primal variable z and the dual variable β, which is common in the convergence rate analysis of the ADMM [23]–[25]. Let us introduce

$$u = \begin{pmatrix} z \\ \beta \end{pmatrix}, G = \begin{pmatrix} cI_{2EN} & 0_{2EN} \\ 0_{2EN} & \frac{1}{c}I_{2EN} \end{pmatrix}. \tag{12}$$

We will show that $u^k = [z^k; \beta^k]$ is Q-linearly convergent to its optimal $u^* = [z^*; \beta^*]$ with respect to the G-norm. Further, the Q-linear convergence of $u^k = [z^k; \beta^k]$ to $u^* = [z^*; \beta^*]$ implies that x^k is R-linearly convergent to its optimal x^*.

Theorem 1. *Consider the ADMM iteration (7) that solves (4). The primal variables x and z have their unique optimal values x^* and z^*, respectively; the dual variable β has its unique optimal value β^* that lies in the column space of M_-^T. Recall the definition of u and G defined in (12). If the local objective functions satisfy Assumption 1 and the dual variable β is initialized such that β^0 lies in the column space of M_-^T, then for any $\mu > 1$, $u^k = [z^k; \beta^k]$ is Q-linearly convergent to its optimal $u^* = [z^*; \beta^*]$ with respect to the G-norm*

$$\|u^{k+1} - u^*\|_G^2 \leq \tfrac{1}{1+\delta}\|u^k - u^*\|_G^2, \tag{13}$$

where

$$\delta = \min\left\{ \frac{(\mu-1)\tilde{\sigma}_{\min}^2(M_-)}{\mu\sigma_{\max}^2(M_+)}, \frac{m_f}{\frac{c}{4}\sigma_{\max}^2(M_+) + \frac{\mu}{c}M_f^2\tilde{\sigma}_{\min}^{-2}(M_-)} \right\} > 0. \tag{14}$$

Further, x^k is R-linearly convergent to x^* following from

$$\|x^{k+1} - x^*\|_2^2 \leq \tfrac{1}{m_f}\|u^k - u^*\|_G^2. \tag{15}$$

Proof. See Appendix. ∎

In Theorem 1, (14) shows that $\|u^{k+1} - u^*\|_G^2$ is no greater than $\frac{1}{1+\delta}\|u^k - u^*\|_G^2$ and hence u^k converges to u^* Q-linearly at a rate

$$\rho \leq \sqrt{\frac{1}{1+\delta}}.$$

A larger δ guarantees faster convergence. On the other hand, $\frac{1}{1+\delta}$ is a theoretical upper bound of the convergence rate, probably not tight. The Q-linear convergence of u^k to u^* translates to the R-linear convergence of x to x^* as shown in (15).

B. Accelerating the Convergence

From (14) we can find that the theoretical convergence rate (more precisely, its upper bound) is given in terms of the network topology, the properties of local objective functions, and the algorithm parameter. The value of δ is related with the free parameter $\mu > 1$, $\sigma_{\max}(M_+)$, $\tilde{\sigma}_{\min}(M_-)$, the strongly convexity constant m_f of f, the Lipschitz constant M_f of ∇f, and the algorithm parameter c.

Now we consider tuning the free parameter μ and the algorithm parameter c to maximize δ and thus accelerate the convergence (i.e., through minimizing $\frac{1}{1+\delta}$ that is indeed an upper bound). From the analysis we will see more clearly how the convergence rate is influenced by the network topology and the local objective functions. For convenience, we define the condition number of f as

$$\kappa_f = \frac{M_f}{m_f}.$$

Recall that $m_f = \min_i m_{f_i}$ and $M_f = \max_i M_{f_i}$. Therefore, κ_f is an upper bound of the condition numbers of the local objective functions. We also define the condition number of the underlying graph $\mathcal{G}_d$ or $\mathcal{G}_u$ as

$$\kappa_G = \frac{\sigma_{\max}(M_+)}{\tilde{\sigma}_{\min}(M_-)} = \sqrt{\frac{\sigma_{\max}(L_+)}{\tilde{\sigma}_{\min}(L_-)}}.$$

With regard to the underlying graph, the minimum nonzero singular value of the extended signed Laplacian matrix L_-, denoted as $\tilde{\sigma}_{\min}(L_-)$, is known as its algebraic connectivity [26], [27]. The maximum singular value of the extended signless Laplacian matrix L_+, denoted as $\sigma_{\max}(L_+)$, has also drawn research interests recently [28], [29]. Both $\sigma_{\max}(L_+)$ and $\tilde{\sigma}_{\min}(L_-)$ are measures of network connectedness but the former is weaker. Roughly speaking, larger $\sigma_{\max}(L_+)$ and $\tilde{\sigma}_{\min}(L_-)$ mean stronger connectedness, and a larger κ_G means weaker connectedness.

Keeping the definitions of κ_f and κ_G in mind, the following theorem shows how to choose the free parameter μ and the algorithm parameter c to maximize δ and accelerate the convergence.

Theorem 2. *If the algorithm parameter c in (14) is chosen as*

$$c = c_t = \frac{2\mu^{\frac{1}{2}} M_f}{\sigma_{\max}(M_+)\tilde{\sigma}_{\min}(M_-)} \tag{16}$$

where

$$\mu = \left(1 + \frac{\kappa_G^2}{2\kappa_f^2} - \frac{\kappa_G}{2\kappa_f}\sqrt{\frac{\kappa_G^2}{\kappa_f^2} + 4}\right)^{-1} > 1, \tag{17}$$

then

$$\delta = \delta_{\mathrm{t}} = \frac{1}{2\kappa_f}\sqrt{\frac{1}{\kappa_f^2} + \frac{4}{\kappa_{\mathrm{G}}^2}} - \frac{1}{2\kappa_f^2} \tag{18}$$

maximizes the value of δ in (14) and ensures that (15) holds.

Proof. Observing the two values inside the minimization operator in (14), we find that only the second term is relevant with c. It is easy to check that the value of c in (16), no matter how μ is chosen, maximizes δ as

$$\delta = \min\left\{ \frac{(\mu-1)\tilde{\sigma}_{\min}^2(M_-)}{\mu\sigma_{\max}^2(M_+)}, \frac{m_f\tilde{\sigma}_{\min}(M_-)}{\mu^{\frac{1}{2}}M_f\sigma_{\max}(M_+)} \right\}. \tag{19}$$

Inside the minimization operator in (19), the first and second terms are monotonically increasing and decreasing with regard to $\mu > 1$, respectively. To maximize δ, we choose a value of μ such that the two terms are equal. Simple calculations show that the value of μ in (17), which is larger than 1, satisfies this condition. The resulting maximum value of δ is the one in (18). ∎

The value of δ in (18) is monotonically decreasing with regard to $\kappa_f \geq 1$ and $\kappa_{\mathrm{G}} > 0$. This conclusion suggests that a smaller condition number κ_f of $f(x)$ and a smaller condition number κ_{G} of the graph lead to faster convergence. On the other hand, if these condition numbers keep increasing, the convergence can go arbitrarily slow. In fact, the limit of δ in (18) is 0 as $\kappa_f \to \infty$ or $\kappa_{\mathrm{G}} \to \infty$. Given δ_{t}, the upper bound of δ, we define the upper bound of the convergence rate as

$$\rho_{\mathrm{t}} = \sqrt{\frac{1}{1 + \delta_{\mathrm{t}}}}.$$

IV. NUMERICAL EXPERIMENTS

In this section, we provide extensive numerical experiments and supplement to validate our theoretical analysis. We introduce experimental settings in Section IV-A and then study the influence of different factors on the convergence rate in Sections IV-B through IV-E.

A. Experimental Settings

We generate a network consisting of L agents and possessing at most $\frac{L(L-1)}{2}$ edges. If the network is randomly generated, we define p, the connectivity ratio of the network, as its actual number of edges divided by $\frac{L(L-1)}{2}$. Such a random network is generated with $\frac{L(L-1)}{2}p$ edges that are uniformly randomly chosen, while ensuring the network connected.

We apply the ADMM to a decentralized consensus least squares problem

$$\min_{\tilde{x}} \sum_{i=1}^{L} \frac{1}{2}\|v_i - U_i\tilde{x}\|_2^2. \tag{20}$$

Here $\tilde{x} \in \mathbb{R}^3$ is the unknown signal to estimate and its true values follow the normal distribution $\mathcal{N}(0, I)$, $U_i \in \mathbb{R}^{3 \times 3}$ is the linear measurement matrix of agent i whose elements follow $\mathcal{N}(0, 1)$ by default, and $v_i \in \mathbb{R}^3$ is the measurement vector of agent i whose elements are polluted by random noise following $\mathcal{N}(0, 0.1)$. In Section IV-D the elements of the matrices U_i need to be further manipulated to produce different condition numbers κ_f of the objective functions. We reformulate (20) into the form of (3) as

$$\min_{\{x_i\}, \{z_{ij}\}} \quad \sum_{i=1}^{L} \tfrac{1}{2}\|v_i - U_i x_i\|_2^2, \tag{21}$$
$$\text{s.t.} \qquad x_i = z_{ij}, \ x_j = z_{ij}, \ \forall (i,j) \in \mathcal{A}.$$

The solution to (20) is denoted by x^* in which the part of agent i is denoted by x_i^*. The algorithm is stopped once $\|x^k - x^*\|_2$ reaches 10^{-15} or the number of iterations k reaches 4000, whichever is earlier.

In the numerical experiments, we choose to record the primal error $\|x^k - x^*\|_2$ instead of $\|u^k - u^*\|_G$ as the latter incurs significant extra computation when the number of agents L is large. But note that $\|x^k - x^*\|_2$ is not necessarily monotonic in k. Let the transient convergence rate be $\rho_k = \frac{\|x^k - x^*\|_2}{\|x^{k-1} - x^*\|_2}$. As ρ_k fluctuates, we report the *running geometric-average* rate of convergence $\bar{\rho}_k$ given by

$$\begin{aligned} \bar{\rho}_k \quad &:= \left(\prod_{s=1}^{k} \rho_s \right)^{1/k} \\ &= \left(\frac{\|x^k - x^*\|_2}{\|x^0 - x^*\|_2} \right)^{1/k} \\ &\le \sqrt{\frac{1}{1+\delta}} \left(\sqrt{\frac{1+\delta}{m_f}} \frac{\|u^0 - u^*\|_G}{\|x^0 - x^*\|_2} \right)^{1/k}, \end{aligned} \tag{22}$$

which follows from (13) and (15). While u^0, u^*, x^0 x^*, and m_f influence $\bar{\rho}_k$, observing

$$\bar{\rho} := \lim_{k \to +\infty} \bar{\rho}_k \le \sqrt{\frac{1}{1+\delta}},$$

we see that their influence diminishes and the steady state $\bar{\rho}$ is upper bounded by $\sqrt{\frac{1}{1+\delta}}$ as ρ is. Throughout the numerical experiments, we report $\bar{\rho}_k$ and $\bar{\rho}$.

In the following subsections, we demonstrate how different factors influence the convergence rate. We firstly show the evidence of linear convergence, and along the way, the influence of the connectivity ratio p on the convergence rate (see Section IV-B). Secondly, we compare the practical convergence rate using the best theoretical algorithm parameter $c = c_{\mathrm{t}}$ in (16) and that using the best hand-tuned parameter $c = c^*$ (see Section IV-C). Thirdly, we check the effect of κ_f, the condition number of the objective function (see Section IV-D). Finally, we show how κ_f, the condition number of the network, as well as other network parameters, influence the convergence rate (see Section IV-E). The numerical experiments are summarized in Table II.

TABLE II

SUMMARY OF THE NUMERICAL EXPERIMENTS

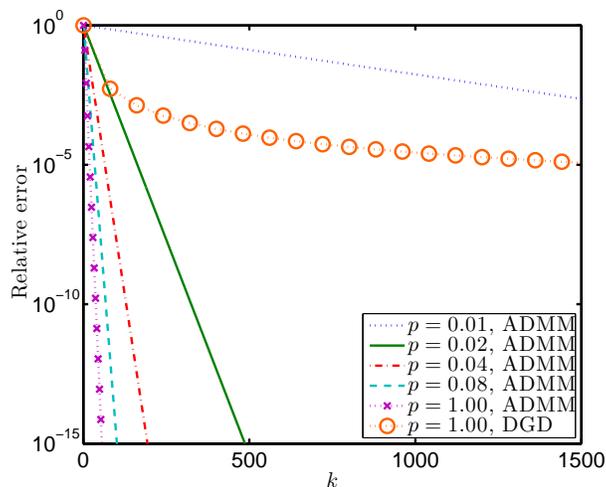| Section	Factor	Conclusion
IV-B	p, connectivity ratio	Larger p leads to faster convergence
IV-C	c, algorithm parameter	$c \simeq 0.5c_{\mathrm{t}}$ works well
IV-D	κ_f, condition number of objective function	Larger κ_f leads to slower convergence
IV-E	κ_{G}, condition number of network	Larger κ_{G} leads to slower convergence
IV-E	D, network diameter	Larger D leads to slower convergence
IV-E	d_s, geometric average degree	Larger d_s leads to faster convergence
IV-E	L_d, imbalance of bipartite graphs	Larger L_d leads to faster convergence

Fig. 1. Relative error $\frac{\|x^k - x^*\|_2}{\|x^*\|_2}$ versus iteration k.

B. Linear Convergence

To illustrate linear convergence of the ADMM for decentralized consensus optimization, we generate random networks consisting of $L = 200$ agents. The connectivity ratio of the networks, p, is set to different values. The ADMM parameter is set as $c = c_{\mathrm{t}}$ (16).

Fig. 1 depicts how the relative error, $\frac{\|x^k - x^*\|_2}{\|x^*\|_2}$, varies in k. Obviously the convergence rates are linear for all p; a higher connectivity ratio leads to faster convergence. Fig. 2 plots $\bar{\rho}_k$, which stabilizes within 10 iterations. From Fig. 1 and Fig. 2, one can observe that for such randomly generated networks, varying the connectivity ratio p within the range $[0.08, 1]$ does not significantly change the convergence rate. The
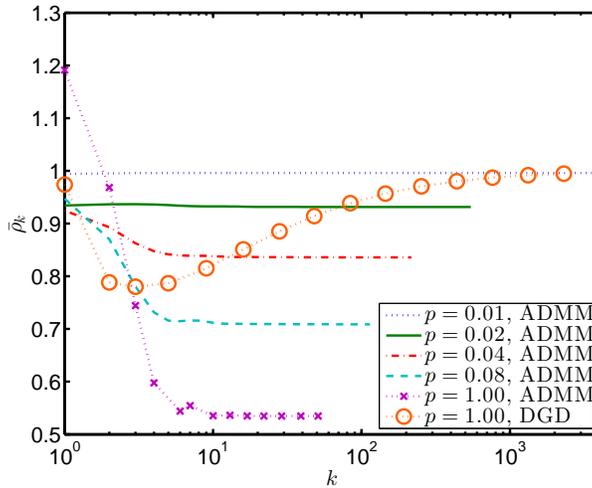
Fig. 2. Running geometric-average rate of convergence $\bar{\rho}_k$ versus iteration k.

reason is that when p is larger than a certain threshold, its value makes little influence on κ_{G} (see Table III in Section IV-C). We will discuss more about the influence of κ_{G} in Section IV-D.

As a comparison, we also demonstrate the convergence of the distributed gradient descent (DGD) method in Fig. 1 and Fig. 2. Using a diminishing stepsize $1/k^{1/3}$ [30], the DGD shows sublinear convergence that is slow even for a complete graph (i.e., $p = 1$).

C. Algorithm Parameter

Here we discuss the influence of the ADMM parameter c on the convergence rate. The best theoretical value $c = c_{\mathrm{t}}$ in (16), though optimizing the upper bound of the convergence rate, does not give best practical performance. We vary c, and plot the steady-state running geometric-average rates of convergence $\bar{\rho}$ in Fig. 3. For each curve that corresponds to a unique p, we mark the best theoretical value c_{t} and the best practical value c^*. Consistently, c_{t} are larger than c^*.

Now we set $c = c^*$, the hand-tuned optimal value, and plot $\frac{\|x^k - x^*\|_2}{\|x^*\|_2}$ in Fig. 4 as per Fig. 1 and $\bar{\rho}_k$ in Fig. 5 as per Fig. 2. Comparing to those using $c = c_{\mathrm{t}}$, the best theoretical value, in Fig. 1 and Fig. 2, the convergence improves significantly. The numerical quantities of Figs. 1, 2, 4, and 5 are given in Table III.

It appears that c_{t} is a stable overestimate of c^*. Therefore, we recommend $c = \theta c_{\mathrm{t}}$ for nearly optimal convergence using some $\theta \in (0, 1)$. Fig. 6 illustrates the convergence corresponding to different values of θ. We randomly generate 4000 connected networks with $L = 200$ agents whose connectivity ratios
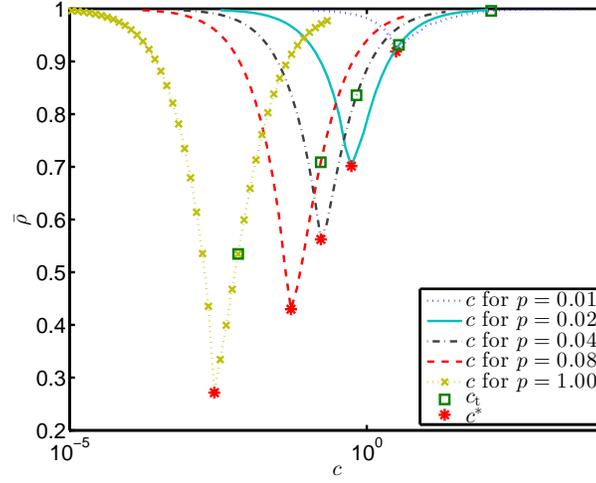
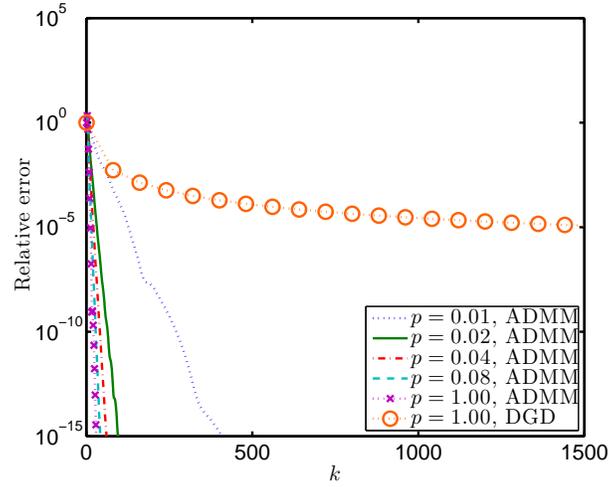Fig. 3. Steady-state running geometric-average rate of convergence $\bar{\rho}$ versus algorithm parameter c.

Fig. 4. Relative error $\frac{\|x^k - x^*\|_2}{\|x^*\|_2}$ versus iteration k.

are uniformly distributed on $[\frac{2}{L}, 1]$. The random networks are divided into 20 groups according to their condition numbers κ_{G}. For each group of the random networks, the values of $\bar{\rho}$ are plotted with error bars, and compared with the theoretical upper bound ρ_{t}. For this dataset, $\theta \simeq 0.5$ appear to be a good overall choice. A smaller θ imposes a risk of slower convergence when κ_{G} is small.
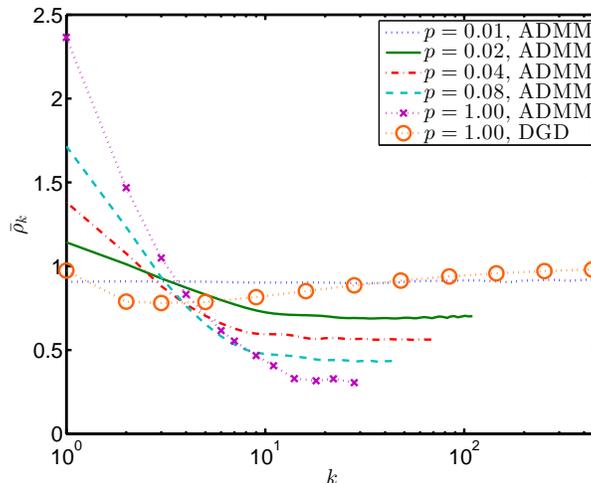
Fig. 5. Running geometric-average rate of convergence $\bar{\rho}_k$ versus iteration k.

TABLE III

SETTINGS AND CONVERGENCE RATES CORRESPONDING TO FIG. 1, FIG. 2, FIG. 4, AND FIG. 5

| Connectivity ratio p | | Best theoretical c_{t} | | Best practical c^* | | Theoretical rate |
$(L = 200$ agents$)$	κ_{G}	c	$\bar{\rho}$	c	$\bar{\rho}$	ρ_{t}
0.01	33.00	123.8	0.9960	3.110	0.9189	0.9908
0.02	7.032	3.477	0.9314	0.5510	0.7014	0.9806
0.04	3.500	0.6714	0.8358	0.1687	0.5624	0.9295
0.08	2.221	0.1677	0.7088	0.05303	0.4297	0.8526
1.00	1.411	0.006837	0.5348	0.002722	0.2714	0.7313

D. Condition Number of the Objective Function

Now we study how κ_f, the condition number of the objective function, affects the convergence rate. We generate random networks consisting of $L = 200$ agents with different connectivity ratios p. We set $c = c_{\mathrm{t}}$. To produce different κ_f, we first generate a linear measurement matrix U_i with its elements following $\mathcal{N}(0, 1)$. Second, we apply singular value decompositions to U_i, scale the singular values to the range $[\sqrt{\frac{1}{\kappa_f}}, 1]$, and rebuild U_i.

Fig. 7 shows that the theoretical convergence rates ρ_{t} are monotonically increasing as κ_f increases, which is consistent with Theorem 2. When the connectivity ratios p are small, the trend of $\bar{\rho}$ disobeys the theoretical analysis. It is because that our upper bound of the convergence rate, becomes loose when
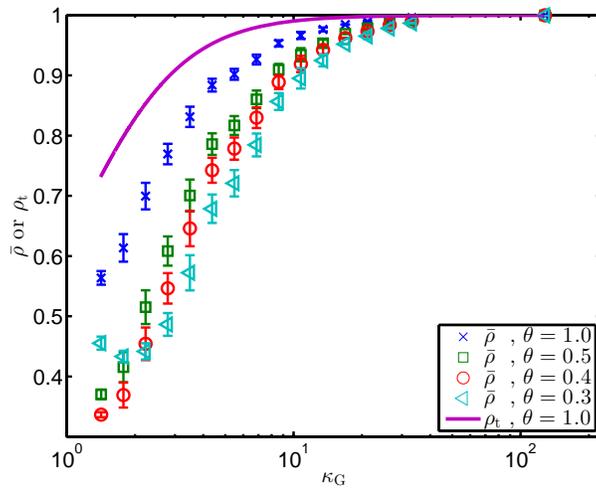
Fig. 6. Convergence performance obtained with $c = \theta c_\mathrm{t}$ for varying θ, where c_t is analytically given in (16).

the network connectedness is poor. When the network is well-connected (say $p = 1$), we can observe a positive correlation between $\bar{\rho}$ and κ_f, which coincides with the theoretical analysis.
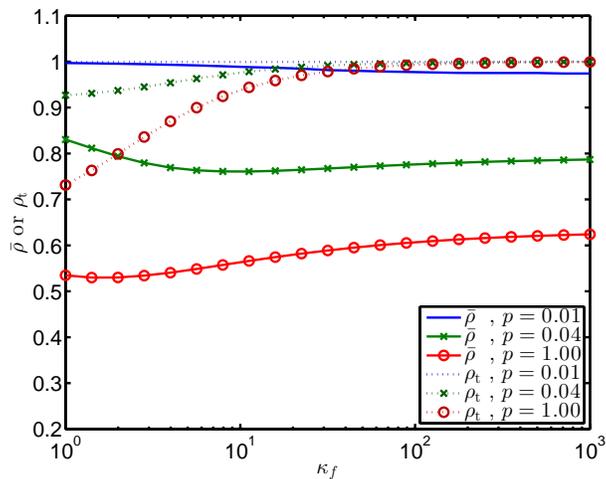

Fig. 7. Convergence performance versus the condition number κ_f of the objective function at different connectivity ratios p.

E. Network Topology

Last we study how the network topology affects the convergence rate. Besides the condition number κ_G of the network that is relevant, we also consider other network parameters including the network diameter,

geometric average degree, as well as imbalance of bipartite networks. In the numerical experiments, the local objective functions are generated as described in Section IV-A. The algorithm parameter is set as $c = c_{\mathrm{t}}$.

1) Condition Number of the Network: As it is difficult to precisely design κ_{G}, the condition number of the network, we run a large number of trials to sample κ_{G}. We randomly generate 4000 connected networks with $L = 50, 200, 500$ agents, 12000 networks in total. Their connectivity ratios are uniformly distributed on $[\frac{2}{L}, 1]$. In addition, we generate special networks with topologies of the line, cycle, star, complete, and grid types. The grid networks are generated in a 3D space ($2 \times 5 \times 5$, $5 \times 5 \times 8$, and $5 \times 10 \times 10$).

Fig. 8 depicts the effect of κ_{G} on the convergence rate. In Fig. 8, the dashed curve with error bars correspond to the random networks, and the individual points correspond to the special networks. There is only one dashed curve in the plot since $L = 50, 200, 500$ do not make significant differences. The networks of the line, cycle, complete, and grid topologies generate points in the plot that are nearly on the dashed curve, which indicates that κ_{G} is a good indicator for convergence rate. In addition, the trends of $\bar{\rho}$, the steady-state running geometric-average rate of convergence, and ρ_{t}, the theoretical rate of convergence, are consistent. The points corresponding to the three networks of the star topology are away from the dashed side.

We observe that the convergence rate is closely related to κ_{G}, less to L. To reach a target convergence rate, one therefore shall have a sufficiently small κ_{G}, which in turn depends on L and p, as well as other factors. To obtain a sufficiently small κ_{G}, typically, p needs to be large if L is small, but not as large if L is large. In other words, if one has a network with a large number of agents (say $L = 200$), a small connectivity ratio (say $p = 0.1$) will lead to a small κ_{G} and thus fast convergence.

With the same κ_{G}, the networks with the star topology have much faster convergence than random networks. We shall discuss this special topology at the end of this subsection.

2) Network Diameter: The network diameter D is defined as the longest distance between any pair of agents in the network. In decentralized consensus optimization, D is related to how many iterations the information from one agent will reach all the other agents.

To discuss the effect of the network diameter on the convergence rate, we randomly generated 4000 connected networks with $L = 200$ agents and connectivity ratios uniformly distributed on $[\frac{2}{L}, 1]$. We also generate the networks of the line, cycle, star, complete, and grid topologies. Most randomly generated networks possess small diameters. In this experiment, the numbers of those with $D = 2$, $3 \leq D \leq 4$ and $5 \leq D \leq 198$ are 3141, 717 and 142, respectively. From Fig. 9, we conclude that in general a larger
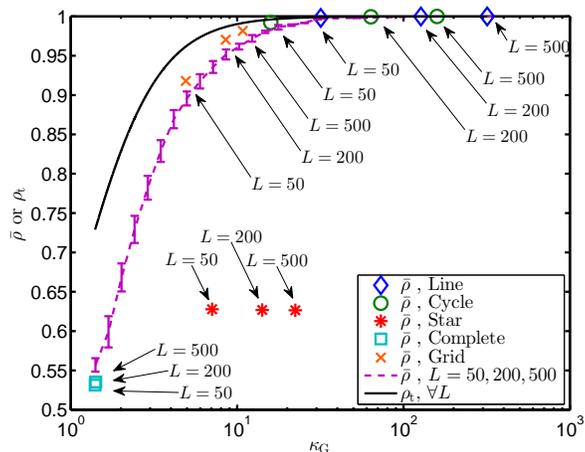
Fig. 8. Convergence performance versus the condition number of the network κ_G obtained with networks of different topologies (random, line, cycle, star, complete, and grid) and of different sizes ($L = 50, 200, 500$).
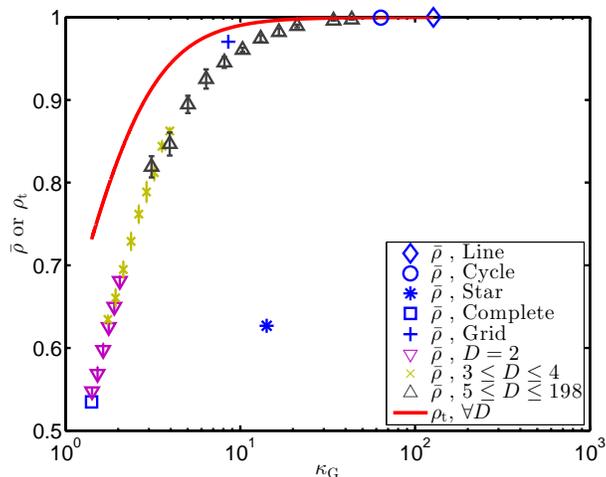

Fig. 9. Convergence performance versus the condition number κ_G of the network and the network diameter D obtained with networks of different topologies (random, line, cycle, star, complete, and grid) and of size $L = 200$.

diameter tends to cause a worse condition number of the network and thus slower convergence, though this relationship is interfered by network properties.

3) Geometric Average Degree: Define $d_{\min}$ and $d_{\max}$ as the largest and smallest degrees of the agents in the network, respectively. The geometric average degree $d_s = \sqrt{d_{\min} d_{\max}}$ reflects the agents' number of neighbors in a geometric average sense. Its value reaches maximum at $L-1$ if the topology is complete;
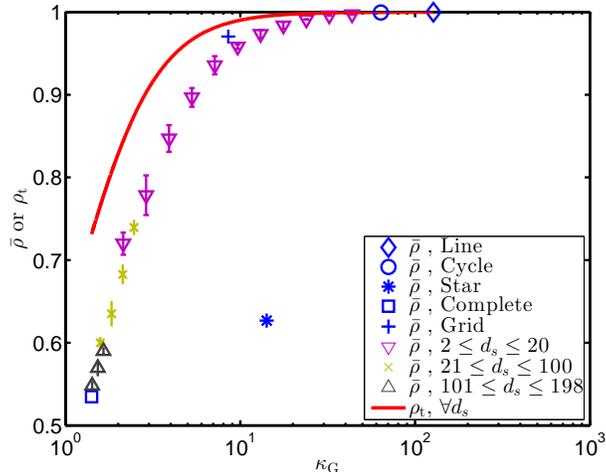
Fig. 10. Convergence performance versus the condition number κ_G of the network and the geometric average degree d_s obtained with networks of different topologies (random, line, cycle, star, complete, and grid) and of size $L = 200$.

and reaches minimum $\sqrt{2}$ when the topology is a line.

Again, we randomly generated 4000 connected networks with $L = 200$ agents and connectivity ratios uniformly distributed on $[\frac{2}{L}, 1]$. We also generate the networks of the line, cycle, star, complete, and grid topologies. Out of the randomly generated networks, 417 have $2 \le d_s \le 20$, 1576 have $21 \le d_s \le 100$, and 1956 have $101 \le d_s \le 198$. From Fig. 10, we observe that a larger d_s generally implies better connectedness and thus a smaller condition number of the network as well as faster convergence. This conclusion is similar to the one on the network diameter D (see Fig. 9).

4) Imbalance of Bipartite Networks: Let $\mathcal{B}(\mathcal{L}_A, \mathcal{L}_B)$ denote the class of bipartite networks with $|\mathcal{L}_A|$ agents in one group and $|\mathcal{L}_B|$ agents in another group. Agents within either group cannot directly communicate with each other. For a bipartite network consisting of $L = |\mathcal{L}_A| + |\mathcal{L}_B|$ agents, its imbalance is defined as $L_d = |\mathcal{L}_A| - |\mathcal{L}_B|$, which can vary between 0 and $L - 2$.

We randomly generate 1000 bipartite graphs of size $L = 200$, whose connectivity ratios p are uniformly distributed on $[\frac{2}{L}, \frac{(L+L_d)(L-L_d)}{2L(L-1)}]$, for each of the cases $L_d = 196, 180, 140, 0$. The star topology corresponds to a special bipartite network with $L_d = L - 2 = 198$. From Fig. 11, we find that for the same κ_G, the networks with larger L_d have faster convergence. An extreme example is the network of the star topology. This observation suggests us to assign few "hot spots" to relay information for fast convergence, if κ_G is fixed in advance. However, this approach may cause robustness or scalability issues because the relaying agents are subject to extensive communication burden. Hence there is a tradeoff
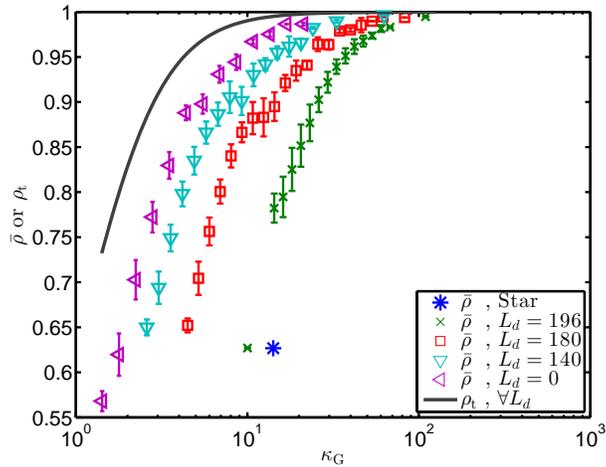
Fig. 11. Convergence performance versus the condition number κ_G of the network and the imbalance of bipartite networks L_d obtained with networks of random and star topologies and of size $L = 200$.

between fast convergence and robustness or scalability in network design.

V. CONCLUSIONS

We apply the ADMM to a reformulation of a general decentralized consensus optimization problem. We show that if the objective function is strongly convex, the decentralized ADMM converges at a globally linear rate, which can be given explicitly. It is revealed that several factors affect the convergence rate that include the topology-related properties of the network, the condition number of the objective function, and the algorithm parameter. Numerical experiments corroborate and supplement our theoretical findings. Our analysis sheds light on how to construct a network and tune the algorithm parameter for fast convergence.

APPENDIX

Proof. Consider the ADMM updates (7) and the KKT conditions (11). Subtracting the three equations in (11) from the corresponding equations in (7) yields

$$\nabla f(x^{k+1}) - \nabla f(x^*) = cM_+(z^k - z^{k+1}) - M_-(\beta^{k+1} - \beta^*), \tag{23}$$

$$\frac{c}{2} M_-^T (x^{k+1} - x^*) = \beta^{k+1} - \beta^k, \tag{24}$$

$$\frac{1}{2} M_+^T (x^{k+1} - x^*) = z^{k+1} - z^*, \tag{25}$$

respectively.

To prove the Q-linear convergence of $\|u^{k+1} - u^*\|_G^2$ we use $m_f \|x^{k+1} - x^*\|_2^2$ as an intermediate. Based on Assumption 1, $f(x)$ is strongly convex with a constant m_f such that

$$m_f \|x^{k+1} - x^*\|_2^2 \leq \langle x^{k+1} - x^*, \nabla f(x^{k+1}) - \nabla f(x^*) \rangle. \tag{26}$$

Using (23), we can split the right-hand side of (26) to two terms

$$
\begin{aligned}
& \langle x^{k+1} - x^*, \nabla f(x^{k+1}) - \nabla f(x^*) \rangle \\
= \ & \langle x^{k+1} - x^*, cM_+(z^k - z^{k+1}) - M_-(\beta^{k+1} - \beta^*) \rangle \\
= \ & \langle x^{k+1} - x^*, cM_+(z^k - z^{k+1}) \rangle + \langle x^{k+1} - x^*, -M_-(\beta^{k+1} - \beta^*) \rangle \\
= \ & c \langle M_+^T(x^{k+1} - x^*), z^k - z^{k+1} \rangle + \langle -M_-^T(x^{k+1} - x^*), \beta^{k+1} - \beta^* \rangle.
\end{aligned}
\tag{27}
$$

Substituting (24) and (25) to (27) we can eliminate the term $x^{k+1} - x^*$ and obtain

$$
\begin{aligned}
& \langle x^{k+1} - x^*, \nabla f(x^{k+1}) - \nabla f(x^*) \rangle \\
= \ & 2c \langle z^k - z^{k+1}, z^{k+1} - z^* \rangle + \tfrac{2}{c} \langle \beta^k - \beta^{k+1}, \beta^{k+1} - \beta^* \rangle.
\end{aligned}
\tag{28}
$$

Recall the definition of u and G defined in (12). It is obvious that the right-hand side of (28) can be written as a compact form $2(u^k - u^{k+1})^T G(u^{k+1} - u^*)$. Using the equality $2(u^k - u^{k+1})^T G(u^{k+1} - u^*) = \|u^k - u^*\|_G^2 - \|u^{k+1} - u^*\|_G^2 - \|u^k - u^{k+1}\|_G^2$, (28) is equivalent to

$$
\begin{aligned}
& \langle x^{k+1} - x^*, \nabla f(x^{k+1}) - \nabla f(x^*) \rangle \\
= \ & \|u^k - u^*\|_G^2 - \|u^{k+1} - u^*\|_G^2 - \|u^k - u^{k+1}\|_G^2,
\end{aligned}
\tag{29}
$$

and consequently using (26)

$$
\begin{aligned}
& m_f \|x^{k+1} - x^*\|_2^2 \\
\leq \ & \|u^k - u^*\|_G^2 - \|u^{k+1} - u^*\|_G^2 - \|u^k - u^{k+1}\|_G^2.
\end{aligned}
\tag{30}
$$

Having (30) at hand, to prove (13) we only need to show

$$\|u^k - u^{k+1}\|_G^2 + m_f \|x^{k+1} - x^*\|_2^2 \geq \delta \|u^{k+1} - u^*\|_G^2, \tag{31}$$

which is equivalent to

$$c \|z^{k+1} - z^k\|_2^2 + \tfrac{1}{c} \|\beta^{k+1} - \beta^k\|_2^2 + m_f \|x^{k+1} - x^*\|_2^2 \geq \delta c \|z^{k+1} - z^*\|_2^2 + \tfrac{\delta}{c} \|\beta^{k+1} - \beta^*\|_2^2. \tag{32}$$

The idea of proof is to show that $\delta c \|z^{k+1} - z^*\|_2^2$ and $\frac{\delta}{c} \|\beta^{k+1} - \beta^*\|_2^2$ are upper bounded by two non-overlapping parts of the left-hand side of (32), respectively.

The upper bound of $\|z^{k+1} - z^*\|_2^2$ follows from (25) that shows $\frac{1}{2} M_+^T(x^{k+1} - x^*) = z^{k+1} - z^*$. Hence we have

$$
\begin{aligned}
& \|z^{k+1} - z^*\|_2^2 \\
= \ & \tfrac{1}{4} \|M_+^T(x^{k+1} - x^*)\|_2^2 \\
\leq \ & \tfrac{1}{4} \sigma_{\max}^2(M_+) \|x^{k+1} - x^*\|_2^2,
\end{aligned}
\tag{33}
$$

where $\sigma_{\max}(M_+)$ is the largest singular value of M_+. To find the upper bound of $\|\beta^{k+1} - \beta^*\|_2^2$, we use two inequalities $\sigma_{\max}^2(M_+)\|z^{k+1} - z^k\|_2^2 \geq \|M_+^T(z^k - z^{k+1})\|_2^2$ and $M_f^2\|x^{k+1} - x^*\|_2^2 \geq \|\nabla f(x^{k+1}) - \nabla f(x^*)\|_2^2$; the latter holds since $f(x)$ has Lipschitz continuous gradients with a constant M_f. Therefore, given the positive algorithm parameter c and any $\mu > 1$ it holds

$$
\begin{aligned}
&c^2\sigma_{\max}^2(M_+)\|z^{k+1} - z^k\|_2^2 + (\mu - 1)M_f^2\|x^{k+1} - x^*\|_2^2 \\
\geq \quad &\|cM_+^T(z^k - z^{k+1})\|_2^2 + (\mu - 1)\|\nabla f(x^{k+1}) - \nabla f(x^*)\|_2^2.
\end{aligned}
\tag{34}
$$

Recall that from (23) $cM_+(z^k - z^{k+1})$ is the summation of $\nabla f(x^{k+1}) - \nabla f(x^*)$ and $M_-(\beta^{k+1} - \beta^*)$. Hence we can apply the basic inequality $\|a + b\|_2^2 + (\mu - 1)\|a\|_2^2 \geq (1 - \frac{1}{\mu})\|b\|_2^2$, which holds for any $\mu > 0$, to (34) and obtain

$$
\begin{aligned}
&c^2\sigma_{\max}^2(M_+)\|z^{k+1} - z^k\|_2^2 + (\mu - 1)M_f^2\|x^{k+1} - x^*\|_2^2 \\
\geq \quad &(1 - \tfrac{1}{\mu})\|M_-(\beta^{k+1} - \beta^*)\|_2^2.
\end{aligned}
\tag{35}
$$

Since by assumption β^0 is initialized such that it lies in the column space of M_-^T, we know that β^{k+1} lies in the column space of M_-^T too; see the ADMM updates (7). Because β^* also lies in the column space of M_-^T, $\|M_-(\beta^{k+1} - \beta^*)\|_2^2 \geq \tilde{\sigma}_{\min}^2(M_-)\|\beta^{k+1} - \beta^*\|_2^2$ where $\tilde{\sigma}_{\min}(M_-)$ is the smallest nonzero singular value of M_-. Therefore from (35) we can upper bound $\|\beta^{k+1} - \beta^*\|_2^2$ by

$$
\begin{aligned}
&c^2\sigma_{\max}^2(M_+)\|z^{k+1} - z^k\|_2^2 + (\mu - 1)M_f^2\|x^{k+1} - x^*\|_2^2 \\
\geq \quad &(1 - \tfrac{1}{\mu})\tilde{\sigma}_{\min}^2(M_-)\|\beta^{k+1} - \beta^*\|_2^2.
\end{aligned}
\tag{36}
$$

Combining (33) and (36), we prove (32). From (33) we have

$$
\begin{aligned}
&\tfrac{c}{4}\sigma_{\max}^2(M_+)\|x^{k+1} - x^*\|_2^2 \\
\geq \quad &c\|z^{k+1} - z^*\|_2^2.
\end{aligned}
\tag{37}
$$

From (36) we have

$$
\begin{aligned}
&\tfrac{c\mu\sigma_{\max}^2(M_+)}{(\mu-1)\tilde{\sigma}_{\min}^2(M_-)}\|z^{k+1} - z^k\|_2^2 + \tfrac{\mu M_f^2}{c\tilde{\sigma}_{\min}^2(M_-)}\|x^{k+1} - x^*\|_2^2 \\
\geq \quad &\tfrac{1}{c}\|\beta^{k+1} - \beta^*\|_2^2.
\end{aligned}
\tag{38}
$$

Summing up (37) and (38) yields

$$
\begin{aligned}
&\tfrac{c\mu\sigma_{\max}^2(M_+)}{(\mu-1)\tilde{\sigma}_{\min}^2(M_-)}\|z^{k+1} - z^k\|_2^2 + \left(\tfrac{\mu M_f^2}{c\tilde{\sigma}_{\min}^2(M_-)} + \tfrac{c}{4}\sigma_{\max}^2(M_+)\right)\|x^{k+1} - x^*\|_2^2 \\
\geq \quad &c\|z^{k+1} - z^*\|_2^2 + \tfrac{1}{c}\|\beta^{k+1} - \beta^*\|_2^2.
\end{aligned}
\tag{39}
$$

Apparently, δ in (14) satisfies

$$
c\|z^{k+1} - z^k\|_2^2 + m_f\|x^{k+1} - x^*\|_2^2 \geq \delta c\|z^{k+1} - z^*\|_2^2 + \tfrac{\delta}{c}\|\beta^{k+1} - \beta^*\|_2^2,
\tag{40}
$$

and consequently (32), which proves (13).

To prove the R-linear convergence of x^k to x^*, we observe that (30) implies $m_f\|x^{k+1} - x^*\|_2^2 \leq \|u^k - u^*\|_G^2$, which proves (15). ∎

REFERENCES

[1] W. Shi, Q. Ling, K. Yuan, G. Wu, and W. Yin, "Linearly Convergent Decentralized Consensus Optimization with the Alternating Direction Method of Multipliers," in *Proceedings of the 38th International Conference on Acoustics, Speech, and Signal Processing*, 2013.

[2] G. Inalhany, D. Stipanovic, and C. Tomlin, "Decentralized Optimization, with Application to Multiple Aircraft Coordination," in *Proceedings of the 41st IEEE Conference on Decision and Control*, 2002.

[3] W. Ren, R. Beard, and E. Atkins, "Information Consensus in Multivehicle Cooperative Control: Collective Group Behavior through Local Interaction," *IEEE Control Systems Magazine*, vol. 27, pp. 71–82, 2007.

[4] B. Johansson, "On Distributed Optimization in Networked Systems," Ph.D. dissertation, KTH, Automatic Control, 2008, QC 20100813.

[5] L. Xiao, S. Boyd, and S. Kim, "Distributed Average Consensus with Least-mean-square Deviation," *Journal of Parallel and Distributed Computing*, vol. 67, pp. 33–46, 2007.

[6] A. Dimakis, S. Kar, M. R. J. Moura, and A. Scaglione, "Gossip Algorithms for Distributed Signal Processing," *Proceedings of the IEEE*, vol. 98, pp. 1847–1864, 2010.

[7] J. Predd, S. Kulkarni, and H. Poor, "A Collaborative Training Algorithm for Distributed Learning," *IEEE Transactions on Information Theory*, vol. 55, pp. 1856–1871, 2009.

[8] G. Mateos, J. Bazerque, and G. Giannakis, "Distributed Sparse Linear Regression," *IEEE Transactions on Signal Processing*, vol. 58, pp. 5262–5276, 2010.

[9] I. Schizas, A. Ribeiro, and G. Giannakis, "Consensus in Ad hoc WSNs with Noisy Links–Part I: Distributed Estimation of Deterministic Signals," *IEEE Transactions on Signal Processing*, vol. 56, pp. 350–364, 2008.

[10] Q. Ling and Z. Tian, "Decentralized Sparse Signal Recovery for Compressive Sleeping Wireless Sensor Networks," *IEEE Transactions on Signal Processing*, vol. 58, pp. 3816–3827, 2010.

[11] J. Bazerque and G. Giannakis, "Distributed Spectrum Sensing for Cognitive Radio Networks by Exploiting Sparsity," *IEEE Transactions on Signal Processing*, vol. 58, pp. 1847–1862, 2010.

[12] J. Bazerque, G. Mateos, and G. Giannakis, "Group-lasso on Splines for Spectrum Cartograph," *IEEE Transactions on Signal Processing*, vol. 59, pp. 4648–4663, 2011.

[13] V. Kekatos and G. Giannakis, "Distributed Robust Power System State Estimation," *IEEE Transactions on Power Systems*, vol. 28, no. 2, pp. 1617–1626, 2013.

[14] L. Gan, U. Topcu, and S. Low, "Optimal Decentralized Protocol for Electric Vehicle Charging," *IEEE Transactions on Power Systems*, vol. 28, no. 2, pp. 940–951, 2013.

[15] A. Nedic and A. Ozdaglar, "Distributed Subgradient Methods for Multi-agent Optimization," *IEEE Transactions on Automatic Control*, vol. 54, pp. 48–61, 2009.

[16] S. Ram, A. Nedic, and V.Veeravalli, "Distributed Stochastic Subgradient Projection Algorithms for Convex Optimization," *Journal of Optimization Theory and Applications*, vol. 147, pp. 516–545, 2010.

[17] K. Tsianos and M. Rabbat, "Distributed Strongly Convex Optimization," in *Proceedings of the 50th Annual Allerton Conference on Communication, Control and Computing*, 2012.

[18] J. Duchi, A. Agarwal, and M. Wainwright, "Dual Averaging for Distributed Optimization: Convergence Analysis and Network Scaling," *IEEE Transactions on Automatic Control*, vol. 57, no. 3, pp. 592–606, 2012.

[19] K. Tsianos, S. Lawlor, and M. Rabbat, "Push-Sum Distributed Dual Averaging for Convex Optimization," in *Proceedings of the 51st IEEE Annual Conference on Decision and Control*, 2012, pp. 5453–5458.

[20] T. Erseghe, D. Zennaro, E. Dall'Anese, and L. Vangelista, "Fast Consensus by the Alternating Direction Multipliers Method," *IEEE Transactions on Signal Processing*, vol. 59, pp. 5523–5537, 2011.

[21] D. Bertsekas and J. Tsitsiklis, *Parallel and Distributed Computation: Numerical Methods*, 2nd ed. Nashua: Athena Scientific, 1997.

[22] M. Rabbat and R. Nowak, "Quantized Incremental Algorithms for Distributed Optimization," *IEEE Journal of Selected Areas in Communications*, vol. 23, pp. 798–808, 2006.

[23] B. He and X. Yuan, "On the $O(1/t)$ Convergence Rate of the Douglas-Rachford Alternating Direction Method," *SIAM Journal on Numerical Analysis*, vol. 50, no. 2, pp. 700–709, 2012.

[24] M. Hong and Z. Luo, "On the Linear Convergence of the Alternating Direction Method of Multipliers," *arXiv preprint arXiv:1208.3922*, 2012.

[25] W. Deng and W. Yin, "On the Global and Linear Convergence of the Generalized Alternating Direction Method of Multipliers," Rice University, Tech. Rep., 2012, CAAM Technical Report TR12-14.

[26] F. Chung, *Spectral Graph Theory*. American Mathematical Soc., 1997, vol. 92.

[27] M. Fiedler, "Algebra Connectivity of Graphs," *Czechoslovake Mathematical Journnal*, vol. 23, no. 98, pp. 298–305, 1973.

[28] D. Cvetkovic, P. Rowlinson, and S. Simic, "Signless Laplacians of Finite Graphs," *Linear Algebra and its Applications*, vol. 423, pp. 155–171, 2007.

[29] Y. Chen and L. Wang, "Sharp Bounds for the Largest Eigenvalue of the Signless Laplacian of A Graph," *Linear Algebra and its Applications*, vol. 433, pp. 908–913, 2010.

[30] D. Jakovetic, J. Xavier, and J. Moura, "Convergence Rate Analysis of Distributed Gradient Methods for Smooth Optimization," in *20th Telecommunications Forum (TELFOR)*. IEEE, 2012, pp. 867–870.